



**A geometric morphometric approach to the study of
variation of shovel-shaped incisors.**

Journal:	<i>American Journal of Physical Anthropology</i>
Manuscript ID	AJPA-2018-00075.R2
Wiley - Manuscript type:	Technical Note
Date Submitted by the Author:	n/a
Complete List of Authors:	<p>Carayon, Delphine; Universite Toulouse III Paul Sabatier Faculte des Sciences et d'Ingenierie, Laboratoire AMIS, UMR 5288 CNRS; Universite de Montpellier Faculte d'Odontologie, Service de Prothèses</p> <p>Adhikari, Kaustubh; University College London, Department of Genetics, Evolution and Environment, and UCL Genetics Institute</p> <p>Montsarrat, Paul; Universite Toulouse III Paul Sabatier Faculte des Sciences et d'Ingenierie, Faculté d'Odontologie</p> <p>Dumoncel, Jean; Laboratoire d'Anthropobiologie Moléculaire et d'Imagerie de Synthèse, UMR 5288 CNRS-Université de Toulouse (Paul Sabatier), Braga, José; AMIS UMR 5288 CNRS, Hominid Evolutionary Biology; University of the Witwatersrand, Institute for Human Evolution</p> <p>Duployer, Benjamin; Centre Inter-universitaire de Recherche et d'Ingénierie des Matériaux, UMR 5085 CNRS-Université de Toulouse (Paul Sabatier)</p> <p>Delgado, Miguel; Consejo Nacional de Investigaciones Cientificas y Tecnicas</p> <p>Fuentes-Guajado, Macarena; University College London Research Department of Genetics Evolution and Environment, Department of Genetics, Evolution and Environment</p> <p>de Beer, Frikkie; South African Nuclear Energy Corporation</p> <p>Hoffman, Jakobus; Pelindaba, Radiation Science</p> <p>Oettlé, Anna; University of Pretoria, Department of Anatomy</p> <p>Donat, Richard; Institut National de Recherches Archéologiques Préventives, St Estève</p> <p>Pan, Lei; Key Laboratory of Vertebrate Evolution and Human Origins of Chinese Academy of Sciences, Institute of Vertebrate Paleontology and Paleoanthropology, Chinese Academy of Sciences, ; Laboratoire d'Anthropobiologie Moléculaire et d'Imagerie de Synthèse, UMR 5288 CNRS-Université de Toulouse (Paul Sabatier), Ruiz-Linares, Andres; University College London, Biology</p> <p>Tenailleau, Christophe; Centre Inter-universitaire de Recherche et d'Ingénierie des Matériaux, UMR 5085 CNRS-Université de Toulouse (Paul Sabatier)</p> <p>Vaysse, Frédéric; Universite Toulouse III Paul Sabatier Faculte des Sciences et d'Ingenierie, Faculté d'Odontologie</p> <p>Esclassan, Rémi; Universite Toulouse III Paul Sabatier Faculte des Sciences et d'Ingenierie, Faculté d'Odontologie</p> <p>Zanolli, Clément; Universite Toulouse III Paul Sabatier, Laboratoire AMIS,</p>

1
2
3
4
5
6
7
8
9
10
11
12
13
14
15
16
17
18
19
20
21
22
23
24
25
26
27
28
29
30
31
32
33
34
35
36
37
38
39
40
41
42
43
44
45
46
47
48
49
50
51
52
53
54
55
56
57
58
59
60

	UMR 5288
Key Words:	shovel-shape incisors, ASUDAS, Procrustes and non-Procrustes superimpositions, virtual anthropology
Subfield: Please select 2 subfields. Select the main subject first.:	Human biology [living humans; behavior, ecology, physiology, anatomy], Primate biology [behavior, ecology, physiology, anatomy]

SCHOLARONE™
Manuscripts

1
2
3 **1 A geometric morphometric approach to the study of variation of shovel-shaped incisors**

4
5
6 3 Delphine Carayon^{1,2}, Kaustubh Adhikari³, Paul Monsarrat^{4,5}, Jean Dumoncel¹, José Braga^{1,6},
7 4 Benjamin Duployer⁷, Miguel Delgado^{8,9}, Macarena Fuentes-Guajardo³, Frikkie de Beer¹⁰,
8 5 Jakobus W. Hoffman¹⁰, Anna C. Oettlé^{11,12}, Richard Donat^{1,13}, Lei Pan^{14,15}, Andres Ruiz-
9 6 Linares^{3,16,17}, Christophe Tenailleau⁷, Frédéric Vaysse^{1,4}, Rémi Esclassan^{1,4}, Clément Zanolli¹.
10
11
12
13

14 8 ¹UMR 5288 CNRS, Université Toulouse III - Paul Sabatier, France

15 9 ²Faculté d'Odontologie, Université Montpellier I, France

16 10 ³Department of Genetics, Evolution and Environment, and UCL Genetics Institute, University
17 11 College London, London, United Kingdom

18 12 ⁴Faculté d'Odontologie, Université Toulouse III - Paul Sabatier, France

19 13 ⁵STROMALab, CNRS ERL 5311, EFS, INP-ENVT, Inserm, Université Toulouse III - Paul
20 14 Sabatier, France

21 15 ⁶Evolutionary Studies Institute and School of Geosciences, University of the Witwatersrand,
22 16 PO WITS, Johannesburg 2050, South Africa

23 17 ⁷Centre Inter-universitaire de Recherche et d'Ingénierie des Matériaux, UMR 5085 CNRS,
24 18 Université de Toulouse III - Paul Sabatier, France

25 19 ⁸Consejo Nacional de Investigaciones Científicas y Técnicas, CONICET, Buenos Aires,
26 20 República Argentina

27 21 ⁹División Antropología, Facultad de Ciencias Naturales y Museo, Universidad Nacional de La
28 22 Plata, La Plata, República Argentina

29 23 ¹⁰Radiation Science Department, South African Nuclear Energy Corporation (Necsa),
30 24 Pelindaba, South Africa

31 25 ¹¹Department of Anatomy, University of Pretoria, South Africa

32 26 ¹²Department of Anatomy, Sefako Makgatho Health Sciences University, South Africa

33 27 ¹³Institut National de Recherches Archéologiques Préventives- St Estève, France

34 28 ¹⁴Key Laboratory of Vertebrate Evolution and Human Origins, Institute of Vertebrate
35 29 Paleontology and Paleoanthropology, CAS, Beijing, China

36 30 ¹⁵State Key Laboratory of Palaeobiology and Stratigraphy, Nanjing Institute of Geology and
37 31 Palaeontology, CAS, Nanjing, China

38 32 ¹⁶Ministry of Education Key Laboratory of Contemporary Anthropology and Collaborative
39 33 Innovation Center of Genetics and Development, Fudan University, Shanghai, China
40
41
42
43
44
45
46
47
48
49
50
51
52
53
54
55
56
57
58
59
60

1
2
3
4
5
6
7
8
9
10
11
12
13
14
15
16
17
18
19
20
21
22
23
24
25
26
27
28
29
30
31
32
33
34
35
36
37
38
39
40
41
42
43
44
45
46
47
48
49
50
51
52
53
54
55
56
57
58
59
60

34 ¹⁷Laboratory of Biocultural Anthropology, Law, Ethics, and Health (Centre National de la
35 Recherche Scientifique and Etablissement Français du Sang, UMR-7268), Aix-Marseille
36 University, Marseille, France

38 Corresponding author: Delphine Carayon (delphinedom.carayon@orange.fr)

41 Keywords: shovel-shape incisors; ASUDAS; Procrustes and non-Procrustes superimpositions;
42 virtual anthropology

1
2
3 56 **Abstract**

4 57 **Objectives:** The scoring and analysis of dental non-metric traits are predominantly
5 58 accomplished by using the Arizona State University Dental Anthropology System
6 59 (ASUDAS), a standard protocol based on strict definitions and three-dimensional dental
7 60 plaques. However, visual scoring, even when controlled by strict definitions of features,
8 61 visual reference and the experience of the observer, includes an unavoidable part of
9 62 subjectivity. In this methodological contribution, we propose a new quantitative geometric
10 63 morphometric approach to quickly and efficiently assess the variation of shoveling in modern
11 64 human maxillary central incisors (UI1).

12 65 **Materials and Methods:** We analyzed 87 modern human UI1s by means of virtual imaging
13 66 and the ASU-UI1 dental plaque grades using geometric morphometrics by placing
14 67 semilandmarks on the labial crown aspect. The modern human sample was composed of
15 68 individuals from Europe, Africa and Asia and included representatives of all seven grades
16 69 defined by the ASUDAS method.

17 70 **Results:** Our results highlighted some limitations in the use of the current UI1 ASUDAS
18 71 plaque, indicating that it did not necessarily represent an objective gradient of expression of a
19 72 non-metric tooth feature. Rating of shoveling tended to be more prone to intra- and inter-
20 73 observer bias for the highest grades. In addition, our analyses suggest that the observers were
21 74 strongly influenced by the depth of the lingual crown aspect when assessing the shoveling.

22 75 **Discussion:** In this context, our results provide a reliable and reproducible framework
23 76 reinforced by statistical results supporting the fact that open scale numerical measurements
24 77 can complement the ASUDAS method.
25
26
27
28
29
30
31
32
33
34
35
36
37
38
39
40
41
42
43
44
45
46
47
48
49
50
51
52
53
54
55
56
57
58
59
60

Introduction

Teeth display morphological variations of the crown and roots that differ substantially among modern human and fossil groups, some dental characteristics being predominant in certain groups or populations (Turner et al., 1991). As stated by Hillson, "human eyes and brain are unsurpassed in discerning tiny differences between objects compared side by side, but it is much more difficult to define a scheme for recording size and shape in such a way that comparisons can be made between hundreds of such objects" (Hillson, 1996: 68). For this reason, since the 19th century, several attempts have been made to classify and assess differences between fossil and extant human populations, at first using detailed descriptive approaches and later elaborating scoring systems (reviewed in Irish and Scott, 2016).

Following the influential early works of Hrdlička (1920) and Dahlberg (1956), who standardized a four grade classification plaque for upper incisor shoveling, some researchers tried to reduce the visual subjectivity by measuring the depth of the lingual fossa. However, they had little success because of issues with the precision of the method (Dahlberg and Mikkelsen, 1947, Carbonell, 1963; Goaz and Miller, 1966; Hanihara, 1969). Later Scott (1973) developed an eight degree scale that was then adapted and integrated by Turner and collaborators (1991) into a formal system for scoring non-metric aspects of dental morphology: the Arizona State University Dental Anthropology System (ASUDAS) (Scott, 1973; Turner et al., 1991; Scott and Turner, 1997). This widely-used standard protocol is based on reference plaster plaques representing the casts of selected teeth showing a gradient of expression of a particular trait (Turner et al., 1991; Scott and Turner, 1997; Scott et al., 2018). Since their initial publication, the number of traits and plaques have increased and some of them have been adapted to the range of variation expressed by fossil hominins (Bailey, 2006; Bailey and Hublin, 2013; Irish et al., 2013; Irish and Scott, 2016). The scoring and analysis of dental non-metric traits currently represents a common diagnostic procedure to highlight ancestry/genetic affinities and investigate human variation in anthropological, paleoanthropological and forensic studies (Turner et al., 1991; Scott and Turner, 1997; Irish, 1998; Irish, 2014a; Irish and Guatelli-Steinberg, 2003; Bailey and Hublin, 2013; Zanolli, 2013; Zanolli et al., 2014; Irish and Scott, 2016). If the observer has been trained by an expert, the ASUDAS approach to morphological characters is easy, fast and reliable, and remains the gold standard technique today (Scott and Irish, 2017; Scott et al., 2018). However, visual scoring, even when controlled by strict definitions of features and the experience of the observer, includes an unavoidable part of subjectivity. In fact, the

1
2
3 assessment of shoveling defined by the ASUDAS method has some major limitations inherent
4 to its definition. The specimens selected to develop the reference grades on the plaque were
5 chosen by qualitative appreciation, which does not necessarily represent the morphological
6 variation in a linear way. This can lead to minimal visual difference between some grades of
7 expression and so to the difficulty experienced by users in classifying the analyzed specimens
8 with regard to the ASUDAS (especially for beginners). In brief, both the selection of the
9 reference teeth when creating the ASUDAS method and the comparison of the dental
10 specimens with the ASUDAS plaques are dependent on observations/palpations and the
11 experience of the observer (i.e., dependent on operator subjectivity). Nichol and Turner
12 (1986) have shown that the intra-observer error when assessing the expression of incisor
13 shoveling is small: 4.1% for more than 1 grade difference and only 2% for presence/absence
14 differences. However, as mentioned by Scott and Turner (1997), "it will probably never be
15 possible to attain 100% concordance in replicated observations of tooth crown and root traits,
16 either by single observers or between observers. The reference plaques developed by
17 Dahlberg, K. Hanihara, Turner, and others have enhanced observational precision but they
18 have not been a panacea for the reasons noted above (i.e., threshold expressions, post-eruptive
19 modifications, surficial noise, varying levels of experience, etc.)" (Scott and Turner, 1997:72).

20
21
22
23
24
25
26
27
28
29
30 Incisor shoveling is one of the non-metric features that has received the most attention
31 from anthropologists as an indicator of relationships among populations and it is frequently
32 used for its taxonomic and phylogenetic relevance (e.g., Scott and Turner, 1997; Bailey and
33 Hublin, 2013; Irish et al., 2013, 2014; Carter et al., 2014). This feature can be defined as the
34 degree of elevation of the mesial and distal lingual marginal ridges on the lingual surface of
35 the maxillary incisors, canines and mandibular incisors, with more pronounced forms
36 enclosing a fossa (Hrdlička, 1920; Dahlberg, 1956; Turner et al., 1991, Scott and Turner,
37 1997). Shoveling is more marked and variable in the upper central and lateral incisors, the
38 former being the polar tooth (Irish and Scott, 2016). Ales Hrdlička (1920) was the first to
39 classify the degree of expression of shovel shaped incisors, assess this variation among
40 several human populations and describe its occurrence in non-human species (Scott and
41 Turner, 1997). Among his findings, he indicated that the prevalence and expression of incisor
42 shoveling showed marked geographic variation in modern human populations, being frequent
43 and strongly expressed in Asia, with a South to North increasing cline, but less frequent
44 and weaker in Africa and Europe (Mizogushi, 1985; Turner, 1990; Kimura et al., 2009). Some
45 workers have attempted to quantify the degree of development of the shoveling with an
46 interval scale. Dahlberg and Mikkelsen (1947) used a Vernier scale with a modified Boley
47
48
49
50
51
52
53
54
55
56
57
58
59
60

1
2
3 Gauge to measure the depth of the incisor lingual fossa in millimeters. Hanihara et al. (1975)
4 measured lingual fossa depth in a Japanese population in order to obtain metrical data to
5 calculate intrafamilial correlations. Taverne et al. (1979) tried to measure various parts of a
6 tooth crown surface by an indirect three-dimensional measurement method using
7 photogrammetry and a Moiré pattern (Mizoguchi, 1985). Also, in a shovel-shaped tooth, the
8 marginal ridges may extend from the incisal edge to the basal eminence and sometimes, in
9 very pronounced cases, the ridges can converge on the eminence. In addition, the two
10 marginal ridges may exhibit different degrees of expression (Mizoguchi, 1985). However,
11 according to Scott and Turner (1997), the mesial and distal marginal ridges are so strongly
12 correlated that they can be considered together as a single trait (Scott and Irish, 2017).
13 Crummett also tried to summarize the main characteristics of incisor shoveling by considering
14 three aspects: the expression of the marginal ridges, the development of a lingual tubercle at
15 the lingual base of the crown, from a small swelling to an independent cusp, and the crown
16 convexity or curvature (Crummett, 1994, 1995). More recently, using X-ray
17 microtomographic imaging, Denton investigated the relationship of these three aspects
18 between the external surface of the incisor crown and the enamel-dentin junction in a limited
19 sample of 10 extant humans (Denton, 2011).

20
21
22 Although the expression of dental non-metric features may be sensitive to environmental
23 or epigenetic factors (Mizoguchi, 2013), it is predominantly determined by genetic factors
24 (Scott and Turner, 1997; Jernvall et al., 2000; Salazar-Ciudad and Jernvall, 2002, 2010; Park
25 et al., 2012). To date, the best known genetically-correlated dental trait is incisor shoveling,
26 which involves a single nucleotide polymorphism (SNP) of the ectodysplasin A receptor gene
27 (*EDAR*), the most likely target of positive selection in Asian populations resulting in marked
28 shovel shaped teeth (Kimura et al., 2009, 2012). However, *EDAR* has pleiotropic effects and a
29 recent study suggested that it was selected in Asian groups for its effect of increasing ductal
30 branching in the mammary gland, thereby amplifying the transfer of critical nutrients to
31 infants via the mother's milk (Hlusko et al., 2018). In this case, the dental phenotypic
32 expression associated with this gene could simply represent a side effect. In any case,
33 shoveling constitutes a critical marker to discriminate between human groups and assess
34 ancestry.

35
36
37 The objective of this contribution is to propose a new and complementary quantitative
38 methodological approach to study the concavity of the palatal surface of UI1, used here as a
39 proxy for the variation of the degree of expression of shoveling. We elaborate a geometric
40 morphometric (GM) method taking the depth and shape of the labial incisor crown aspect

1
2
3 (i.e., two of the three aspects of shoveling: the expression of the marginal ridges and the
4 curvature of the lingual aspect) into account to assess the degree of UI1 shoveling on a
5 continuous scale. After comparison with the classical ASUDAS method, we discuss the
6 implications of implementing such geometric morphometric analyses for the study of the
7 modern human variability of dental traits and to better track evolutionary trends in hominins.
8
9
10

11 **Material and methods**

12 *Sample and scanning procedures*

13
14
15 Our sample consisted of 87 modern human permanent maxillary central incisors (UI1). It
16 included specimens of European (n=44), South African (n=30) and Chinese (n=13) ancestry,
17 as listed in Table 1. Only unworn to moderately worn tooth crowns (reaching maximum stage
18 2 as defined by Smith, 1984, and corresponding to a thin line of dentine exposure) having no
19 particular damage or pathology on the labial aspect were included in the analyses. Visual
20 scoring of the 87 specimens was achieved by two observers (DC and CZ) following the
21 ASUDAS method (Supporting Information Table 1).
22

23
24 We also analyzed the original ASUDAS UI1 shoveling (ASU-UI1) plaque based on
25 Dahlberg's work (1956) and developed by Turner and collaborators (1991). This plaque
26 includes seven grades of shoveling expression, from the weakest (grade 0) to the most marked
27 (grade 6) (Supporting Information Table 2). In a recent revision of the ASUDAS method,
28 Scott and Irish (2017) described an 8th stage for UI1 shoveling (grade 7, defined as any
29 expression that exceeds grade 6, involving marginal ridges that fold around on themselves,
30 similar to grade 6 on the UI2 shoveling plaque) but they did not find any suitable example to
31 put on the plaque. For this reason, we did not consider this last grade here.
32
33
34
35
36
37
38
39

40 The 44 European specimens were scanned by X-ray microtomography (micro-CT) at the
41 CIRIMAT facility of the University of Toulouse with a Phoenix/GE Nanotom 180 instrument,
42 using the following parameters: 100 kV, 100 μ A, 0.36° angular step. The virtual records were
43 reconstructed to a voxel size of 22 to 25 μ m. The 30 South African teeth and the reference
44 plaque ASU-UI1 were scanned by X-Ray Micro-CT at the MIXRAD facility of the South
45 African Nuclear Energy Corporation SOC Limited (Necsa), with a Nikon XT H225-L
46 instrument by using similar parameters, and reconstructed to a voxel size ranging from 42 to
47 50 μ m (Hoffman and de Beer, 2012). The 13 modern human Asian teeth were scanned by X-
48 Ray micro-CT using similar parameters at the Institute of Vertebrate Paleontology and
49 Paleoanthropology of Beijing, China, and reconstructed to a voxel size of 31.4 μ m.
50
51
52
53
54
55
56
57
58
59
60

1
2
3 Data were imported into the 3D analytical software Avizo v.8.0. (FEI Visualization
4 Sciences Group) so that 3D renderings of the tooth external surface could be visualized and
5 processed. Teeth were first segmented semi-automatically by using a thresholding approach
6 (Spoor et al., 1993; Fajardo et al., 2002; Coleman and Colbert, 2007) and a surface was
7 generated from the segmented object. The maximum of curvature was measured on each UI1
8 crown surface using the "MaxCurvature" module of Avizo. This allowed us to determine the
9 extreme curvature line of the mesial and distal lingual crests and use these maxima as starting
10 and ending points of our GM analyses. The cervical best fit plane was defined by placing at
11 least three landmarks at the most apical points of the cervix on the labial and palatal aspects
12 (points of maximum curvature on the labial and lingual sides of the cement enamel junction;
13 Le Cabec et al., 2013). We translated this reference plane to the midpoint between the most
14 incisal and the most cervical points of the crown (Figure 1a) and then placed 100
15 semilandmarks along this middle plane following the curve of the lingual aspect of the crown
16 (Figure 1b).

27 *Statistical analysis*

28
29 Intra-observer error (reliability) of the ASUDAS visual scoring was assessed with respect
30 to the UI1 reference plaque by intra-class correlation (ICC) using a two-way mixed effects
31 "absolute agreement" model (Koo and Li, 2017). ICC is generally used to assess the
32 correlation of various units organized in groups and describes how strongly units in the same
33 group resemble each other. This analysis was done in order to check for both consistency
34 (also referred to as precision in the literature; e.g., if a tooth is actually ASUDAS category 2,
35 but two raters independently assign it to category 5, they are highly consistent with each other
36 but they have a large bias of 3 units; Schrouf and Fleiss, 1979; Joint Committee for Guides in
37 Metrology, 2008; Hughes and Hase, 2010) and accuracy (i.e., looking for the degree of
38 bias/error between observers and our objective landmark-based method, e.g., if grade 3
39 actually corresponds to grade 3 plaque).

40
41 To objectively compare the degree of concavity of the labial surface of each incisor from
42 our sample with the grades of the reference plaque, we performed Procrustes analyses of the
43 semilandmarks. In the Procrustes method, the original landmarks from all samples are first
44 superimposed and aligned with one another to produce the Procrustes coordinates.
45 Subsequently, a principal component analysis (PCA) of the Procrustes coordinates is
46 performed.

1
2
3 The reliability of this computer-based technique was assessed by intra-class correlation
4 (ICC) of the 100 landmark coordinates among the three operators and 30 samples. Reliability
5 was higher when the distance between the landmarks assigned by two raters on the same
6 sample was small. We considered the distance between the landmark and the origin of the 3D
7 orthonormal reference as outcome, together with the individual X, Y and Z float coordinates.
8 ICC was obtained after a two-way random effects “absolute agreement” model (Koo and Li,
9 2017). Levels of agreement between raters were also visually appreciated using Bland-Altman
10 plots. (This kind of plot, assessing the degree of agreement between two observers, is similar
11 to a Tukey mean-difference plot.)
12
13
14
15
16

17 We also superimposed the curves in a non-Procrustes way, aligning the first and last point
18 (0 and 100 respectively) of each curve (Figure 2a). This alignment procedure requires an
19 initial 3D rotation step, which is similar to Procrustes methods, but the subsequent steps are
20 different from Procrustes. Since each curve lies in an approximate 3D plane (the
21 semilandmarks are placed along a plane, see Figure 1b), the curve is rotated to approximately
22 align with the X-Y plane (equation of the 3D plane is obtained by fitting a linear regression on
23 the X, Y & Z coordinates, as the equation of a 3D plane is $aX + bY + cZ + d = 0$). After this
24 alignment, the Z coordinate is discarded. The 2D data is then rotated again so that the first and
25 last points lie on the Y axis (i.e. X coordinate = 0). Finally, they are scaled by a constant
26 factor on both axes to achieve a fixed Y-axis range of 1, i.e. the first and last points of each
27 curve now have coordinates (0,0) and (0,1) respectively. This scaling step is a major
28 difference from the Procrustes method, as the classical Procrustes method scales to have a
29 centroid size of 1, but here the curves are scaled to have a Y-axis range of 1 to facilitate
30 comparisons. We then used these aligned coordinates to measure two metrics, the maximum
31 depth of the lingual aspect with respect to the first and last points of the curves and the hollow
32 area of the curves (Figure 2b). These metrics are not data-dependent like the previous one (PC
33 scores have to be calculated in the whole sample, and values change according to the sample
34 composition) as both the depth and hollow area can be measured directly on the aligned
35 landmarks. Principal components were also calculated from the non-Procrustes aligned
36 coordinates (X & Y).
37
38
39
40
41
42
43
44
45
46
47
48
49

50 All statistical analyses and graphic data visualization were performed in MATLAB
51 R2017b (MATLAB and Statistics Toolbox Release, R2017b) and R 3.4.3 (R Core Team,
52 2018). The following R packages were used: scatterplot3d (Ligges and Mächler, 2003),
53 shapes (Dryden, 2017), ade4 (Dray and Dufour, 2007), irr (Gamer et al., 2012) and Bland
54 Altman Leh (Lehnert, 2015).
55
56
57
58
59
60

1
2
3 Most morphological variations in the human dentition vary on a continuous scale.
4 However, for simplicity of representation, dental anthropological assessment schemes often
5 use two or more categories into which the range of variation is 'binned' or 'categorized'. For
6 instance, the amount of melanin pigmentation in the eye is a continuous quantity, but in
7 traditional analyses it has been categorized into blue vs. brown to represent absence/presence
8 of melanin, and historically considered to be a Mendelian trait until modern quantitative
9 analysis showed its complex polygenic nature. Scott and Turner (1997) noted, specifically
10 with the example of incisor shoveling, that such nonmetric dental traits are possibly 'quasi
11 continuous' (ordinal or dichotomous) traits, derived from an underlying continuous trait. For
12 example, while the depth of the incisor crown is a continuous quantity, it can be dichotomized
13 into absence/presence indicating whether the amount of curvature is below a certain threshold.
14 In such cases, the underlying continuous variable is called a 'latent variable' corresponding to
15 the assessed categorical variable. Our analyses suggested that the maximum depth metric was
16 the most likely candidate for any underlying 'latent' quantitative variable that might be the
17 basis of the ASUDAS categories for shoveling (see Results below). The results also suggested
18 that the relationship between the maximum depth variable and the ASUDAS categories was
19 monotonic but non-linear, i.e. when the latent variable increases the categories also increase,
20 but the spacing between categories is unequal. Therefore, to 'predict' an objective ASUDAS
21 category for the 87 modern human specimens, we constructed a prediction function using the
22 maximum depth values and numerical categories of the ASUDAS specimen teeth. To
23 preserve nonlinearity, a spline function was fitted on these values, which was then used as the
24 interpolant to obtain predicted ASUDAS categories from the 3-D measured maximum depth
25 values on the 87 modern human specimen casts. The predicted ASUDAS categories were
26 allowed to contain decimals to retain more precision, instead of rounding them off to the
27 nearest integer category (e.g., 1.67 instead of 2). Similarly, some of the observer-assigned
28 categories that had an intermediate rating (0_1 meaning a category between ASUDAS
29 references 0 and 1) were allowed to retain them (the rating 0_1 was assigned the middle value
30 of 0.5, for example). These objective predicted values were compared with subjective
31 observer-assigned rating values via ICC to obtain accuracy (i.e. unbiasedness) measurements.
32
33
34
35
36
37
38
39
40
41
42
43
44
45
46
47
48
49

51 Results

52 Our ICC intra- and inter-observer tests on the visual scoring showed highly consistent
53 assessment of shoveling within and between raters (Table 2). Consistency was high for the
54 whole sample, but also for each chrono-geographic sub-sample considered in this study. In
55
56
57
58
59
60

1
2
3 contrast, the accuracy of the visual assessment performed by the raters, measured using the
4 ICC between the rater-assigned category and the predicted category was moderate for the
5 Europeans and Africans. For the Chinese sample, the accuracy of the visual assessment was
6 very low (further discussion below).
7
8

9 We then looked at the results of the landmark-based analyses. Following the standard
10 procedure in geometric morphometrics, principal component analysis (PCA) was used to
11 explore the morphospace. Principal components (PCs) were calculated using the Procrustes
12 coordinates of all landmarks, for all samples including the ASUDAS reference casts. Plotting
13 the top PCs enabled us to visualize the morphospace, to see how the samples were distributed
14 with respect to the ASUDAS grades (Figure 3). The first two components (PC1 and PC2) of
15 the PCA accounted for 87.4% of the total variance (81.5% for PC1 and 5.9% for PC2).
16
17
18
19

20 PC shape changes could be visualized by plotting the PC loadings. PC loadings for the
21 Procrustes and non-Procrustes methods were very similar; non-Procrustes PC shape changes
22 are shown in Supporting Information Figure 1. While PCs are more difficult to interpret than
23 direct measurements, the PC shape changes give us some idea of the morphological aspects
24 they capture. The shape of PC1 is roughly proportional to the curve of the lingual aspect, i.e.
25 the lingual fossa has the highest weight. Therefore the deeper the lingual fossa is from the
26 baseline, the higher the PC value is. This explains why the PC has such high correlations with
27 the maximum depth metric (Table 3). And since the deeper the lingual fossa is, the more the
28 marginal ridges protrude with respect to the fossa, PC1 is also proportional to the ASUDAS
29 shoveling grade (Table 4).
30
31
32
33
34
35
36

37 The shape of PC2 gives greatest weight to the corners of marginal ridges, thereby being
38 proportional to the angle between the labial palate and the marginal ridges. This angle is
39 called 'labial convexity' in Denton (2011), where it is shown that its relationship with the
40 ASUDAS shoveling grade is not monotonic (largest angles for grades 2-3), which explains
41 why PC2 is not strongly correlated with it (Table 4).
42
43
44

45 The shape of PC3 seems to reflect the left-right asymmetry present in the shape of the
46 curve, in particular the asymmetry in the two angles. As asymmetry of the ridges is not
47 relevant in the definition of the ASUDAS grades, this explains why PC3 is not correlated with
48 the grades either (Table 4).
49
50

51 The shapes of later PCs, such as PC4, are much harder to interpret and, given that they
52 capture a very small fraction of the variability, they might simply reflect random statistical
53 variation.
54
55
56
57
58
59
60

1
2
3 Along PC1, the European (French contemporary and medieval) and South African
4 specimens showed a similarly reduced expression of shoveling (expressed here by reduced
5 lingual depth and a more linear morphology), overlapping with the ASUDAS grades 0 and 1,
6 while the Chinese material encompassed the grades 2 to 5. Even though the ASUDAS grades
7 tend to follow a trend along PC1, their distribution is not linearly organized and is
8 heterogeneous (Figure 3a and Figure 4a). Grades 0-1, 2-3, 4-5 and 6 tended to form four
9 clusters and grades were not equidistant from one another. There was no visible
10 discrimination between the chrono-geographic human samples and the ASUDAS grades
11 along PC3 and PC4, which represented 3.16% and 2.55%, respectively, of the total variance
12 (Figure 3b). We tested the reproducibility of this Procrustes method. Our results show that the
13 positioning of the landmarks was highly reproducible, with an ICC >0.990. The graphical
14 Bland-Altman method confirmed this high level of agreement (Figure 5).

15
16
17
18
19
20
21
22 When considering the Non-Procrustes analysis, similar results were obtained. In Figure 4,
23 the histograms showing the distribution of maximum depth (Figure 4b) and hollow area
24 (Figure 4c) of the specimens and the ASUDAS grades also highlight the non-linear scattering
25 of the reference grades. Again, grades 0 and 1 are close to each other, while grades 2 to 5 are
26 grouped together and 6 is alone. In accordance with the knowledge that East Asian
27 populations show a higher degree of shoveling than the rest, the histogram of Chinese samples
28 for maximum depth (Figure 4b) shows no overlap with the French and South African samples.
29 It is also interesting to note that several samples from each population have a maximum depth
30 value that is intermediate between the ASUDAS categories 1 & 2 (which have a large gap
31 between them). This might create some difficulties for the observers to assign ASUDAS
32 ratings to them, and also reduce the distinction between populations when compared via
33 ASUDAS category frequencies. However, the quantitative maximum depth measurements
34 provide a complete separation of the Chinese samples from the rest. The hollow area metric
35 also achieves near-complete separation and shows a similar pattern.

36
37
38
39
40
41
42
43
44
45 Principal components calculated from the non-Procrustes aligned coordinates showed
46 trends similar to those of the Procrustes PCs. PC1 alone explained 92% of the variation, while
47 PC2 explained a further 2.7%. The PC loadings are represented as PC shape changes in
48 Supporting Information Figure 1.

49
50
51
52
53
54
55
56
57
58
59
60 Table 3 presents the correlation between these various metrics calculated on the 87 human
specimens plus the 7 ASUDAS reference casts. In addition to the two direct measurements,
maximum depth and hollow area, PC1 and PC2 are used from both Procrustes and non-
Procrustes aligned methods. This indicates that the two direct metrics are very similar to each

1
2
3 other, so it is sufficient to use either one. It also shows that both direct metric measurements,
4 maximum depth and hollow area, have very high correlation with PC values obtained from
5 the two analyses, as expected from the observations above, and therefore can be used in lieu
6 of Procrustes PC values. The advantage of using direct measurement metrics over Procrustes
7 PCs is that they are more directly interpretable, and not dependent on the whole dataset.
8
9

10
11 The correlation of ASUDAS category values with these metrics calculated on the
12 ASUDAS reference casts was also assessed (Supporting Information Table 3). It shows that
13 both metrics, as well as PC1 from both analyses, are highly correlated with the category
14 values, while maximum depth has the highest correlation (98%). It also indicates that the
15 Procrustes and non-Procrustes PCs are very similar to each other. The major feature of the
16 ASUDAS scale for shoveling is the progressively increasing expression of the marginal ridges
17 (Scott and Turner, 1997; Scott and Irish 2017). Conversely, more protruding ridges imply a
18 deeper lingual fossa, and hence the maximal depth metric gives a measure of the development
19 of the mesial and distal ridges and constitutes an appropriate metric to quantitatively evaluate
20 the expression of shoveling.
21
22
23
24
25
26

27 When combining the correlation patterns with the observation above that the maximum
28 depth metric provides a complete separation of the Chinese samples from the rest, we
29 considered the maximum depth to be the most likely candidate for any underlying ‘latent’
30 quantitative variable that might be the basis of the ASUDAS categories. Considering that
31 maximum depth has a 99% correlation with non-Procrustes PC1, which explains 92%
32 variation of the landmark coordinates, it can be said that the maximum depth metric captures
33 a large part of the morphological variation of the labial aspect of the U11 crown.
34
35
36
37

38 To assess the accuracy of the visual ASUDAS assessments made by two observers, we
39 needed to compare them with objective ‘true’ assessments of the modern human specimens.
40 To make such objective estimates of ASUDAS categories on the specimens, we started with
41 the objectively measured maximum depth metric, and employed the previously described
42 prediction function. The prediction procedure uses the spline interpolation function
43 constructed entirely on the basis of the ASUDAS reference plaque (Figure 6), and is therefore
44 free of subjectivity arising from other human raters. The spline model compares the maximum
45 depth measurements against ASUDAS categories for the ASUDAS reference plaque
46 elements. Using this objective prediction function on the objectively measured maximum
47 depth metric for a new specimen provides an objective estimate of the ASUDAS grade for the
48 new specimen. This estimated grade can then be compared to the subjective ASUDAS ratings
49 provided by a human observer in order to assess the accuracy of the observer.
50
51
52
53
54
55
56
57
58
59
60

1
2
3 As found in our ICC intra- and inter-observer tests (Table 2), the specimens the observers
4 assessed as expressing low degrees of shoveling (grades 0-1), namely most of the South
5 African and French samples, were closer to the predicted 'true' values (using the ASUDAS
6 reference grades), being less scattered around the spline interpolation curve used for the
7 prediction (Figure 6). In contrast, observer ratings for those recorded as having marked
8 shoveling (grade 2 and above) – primarily the Chinese samples – were much more scattered
9 around the spline curve, indicating that they differed more from the predicted 'true' ASUDAS
10 grades (Figure 6). This corroborates our observation above that the populations are harder to
11 separate on the categorical ASUDAS scale than by means of the quantitative maximum depth
12 metric. Still, no Chinese specimen was visually rated below grade 2, and very few European
13 and African specimens were recorded as grade 2 or above, which indicates that, despite the
14 subjective variability, the samples can usually be dichotomized by human raters into high or
15 low shoveling with reasonable accuracy.
16
17
18
19
20
21
22
23

24 When comparing the correlation between the visual assessments (based on the ASUDAS
25 definition and plaque) and some objectively obtained measurements (e.g., predicted ASUDAS
26 values, maximum depth, hollow area), we found that the maximum depth and hollow area
27 metrics correlated highly with visual scoring, even to a higher level than with the predicted
28 ASUDAS values (Table 4). This could suggest that there is a major unconscious reaction to
29 the maximum depth aspect when recording shoveling by following the classical ASUDAS
30 method. In order to test whether the observers were more influenced visually by the depth of
31 the palatal aspect than by the global morphology, we dichotomized the observer ratings
32 following the standard protocol for ASUDAS traits (Scott and Irish, 2017, Scott et al., 2018),
33 which splits the categories of this trait into two broad groups (grades ≤ 1 vs. grades ≥ 2), and
34 re-ran ICC consistency and accuracy measures (Table 5). This grouping mimicked the
35 distinction between East Asians and the rest by separating absent/low degrees of shoveling
36 and marked shoveling. The new ICC values showed high degrees of precision and accuracy,
37 suggesting that the visual scoring performed by observers was largely successful at separating
38 low degrees of shoveling from marked shoveling, but not so successful in detecting finer
39 differences between the ASUDAS casts. This result is relevant as it shows that, while the
40 ASUDAS method is efficient to distinguish below and above the breakpoint grade 2, it is
41 more prone to bias when dealing with close grades and limits the possibilities for more
42 advanced analyses. For example, an important question regarding dental traits is to find which
43 genetic factors are responsible for a trait's expression. Scott and Turner (1997) used the
44 example of incisor shoveling to conclude that such nonmetric dental traits possibly arise from
45
46
47
48
49
50
51
52
53
54
55
56
57
58
59
60

1
2
3 an underlying continuous trait which is likely polygenic. They also note that dichotomizing
4 such traits leads to the loss of a large amount of variation in the trait. As an extreme example,
5 all Native Americans may have the constant value of 'present' for the shoveling trait, which
6 causes it to "lose its status as a nonmetric variant as it is present in all individuals." Such loss
7 of variation, either when constructing a 'quasi continuous' (ordinal) trait from a continuous
8 underlying trait, or when dichotomizing an ordinal trait, reduces the resolution of the data.
9 This loss of variation leads to a loss of power in genetic association analysis, where the use of
10 a continuous trait can entail 'significantly higher power', especially with small sample sizes
11 (Bhandari et al., 2002). In their literature review, Scott et al. (2018) also note that such
12 simplifications can create several problems for genetic analyses, e.g. the simplified traits can
13 "sometimes mimic the segregation patterns of simple Mendelian inheritance where, in reality,
14 inheritance is complex." (Scott et al., 2018:133). Even in the context of assessing rater
15 reliability, the higher resolution offered by continuous data provides much better reliability
16 estimates (Donner and Eliasziw, 1994).

17
18 In the context of clinical studies, Altman (2006) comments that dichotomized variables
19 often appear to be more alluring as they simplify the data while retaining the main dichotomy
20 that is thought to be the crux of the variable, thereby leading to simpler interpretations as well
21 as higher rater agreement. Yet such deliberate discarding of data causes several problems: loss
22 of power, increased risk of false positives, underestimation of variation within or between
23 groups, loss of information about the relationship between the trait and other variables, and
24 increased confounding with other variables in regression analysis, such as genetic association
25 analysis. MacCallum et al. (2002) report similar criticisms, and emphasize the problems in
26 statistical analysis. Using a dichotomous variable means that many statistical procedures are
27 not applicable, e.g., in a genetic association study, the standard linear regression model, which
28 allows estimation of effect sizes in absolute units, cannot be used. Dichotomous variables can
29 only be used with logistic regression, which only estimates effect sizes on an odds ratio scale,
30 making it much more difficult to interpret the effect of a genetic marker or combine evidence
31 from multiple studies.

32
33 The sample-dependent nature of Principal Components means that the PCs depend on the
34 whole sample composition. We investigated how the PCs could change when the dataset was
35 limited to European samples, which span only a narrow range of the trait variability (without
36 any marked shoveling). To assess this, we performed the alignment and PC calculation steps
37 for both Procrustes and non-Procrustes methods while restricting the dataset to French
38 samples (contemporary and medieval), and obtained their correlation with the directly
39
40
41
42
43
44
45
46
47
48
49
50
51
52
53
54
55
56
57
58
59
60

1
2
3 measured metrics. For these correlation values, the correlation of PC1 from both analyses
4 with maximum depth decreased a little (compared to Table 3), especially for the Procrustes
5 PC (Supporting Information Table 4). This indicates that PCs calculated in this reduced
6 dataset with a narrower range of variability might have some increased noise or may be
7 slightly less able to capture the actual underlying metric of lower grades. To verify this, we
8 looked at the correlation of rater-assigned ASUDAS categories of the French samples with
9 these PCs and directly measured metrics (Supporting Information Table 5). In contrast to
10 Table 4, correlations of the rater-assigned ASUDAS categories with maximum depth are
11 higher than their correlations with PC1 by a larger margin.
12
13
14
15
16
17
18

19 **Discussion**

20 In the literature, the significance of errors due to the role of the observer in the visual scoring
21 of dental non-metric traits using the ASUDAS method is usually considered as being low
22 and/or negligible (Scott and Turner, 1997; Bailey and Hublin, 2013; Hillson, 2005). Applied
23 to decades of research, the classical ASUDAS method has proved to be quite efficient for
24 inferring biological relationships among modern humans (Scott and Turner, 1997; Scott et al.,
25 2018), living non-human primates (Pilbrow, 2003) and fossil hominins (Mizoguchi, 1985;
26 Crummet, 1994; Bailey and Hublin, 2013; Irish et al., 2013; Bailey and Wood, 2007;
27 Martinon-Torres et al., 2007) – in part because, once the grades are scored, they are
28 dichotomized into presence/absence to help reduce observer error and because of the current
29 dichotomous biological distance statistics available (e.g., MMD). There has been a previous
30 attempt to link morphology and measurements for the UI1 shoveling trait, notably by
31 considering the depth of the lingual fossa with respect to ASUDAS grades (Hanihara, 2008).
32 However, this method only considers the maximum depth at the center of the lingual fossa
33 and does not quantify the shape of this fossa. Thus, it is still possible to develop innovative,
34 complementary methods. The recent development of quick and efficient methods for
35 acquiring 3D models of an object (e.g., photogrammetry, laser scanner), together with the
36 advent of powerful quantitative techniques to assess shape variation (geometric
37 morphometrics), has opened up new ways to test the reliability (precision and accuracy) of the
38 ASUDAS method. These methods represent an opportunity to provide objective protocols to
39 investigate non-metric dental variation. In this preliminary study, we have compared the
40 classical plaque-based visual scoring assessment with a new 3D geometric morphometric
41 approach. We propose here a simple, fast method based on geometric morphometrics to
42 characterize a sample of modern human UI1s using a continuous scale of morphological
43
44
45
46
47
48
49
50
51
52
53
54
55
56
57
58
59
60

1
2
3 variation of shoveling. The intra-observer error related to the visual scoring is very low, as
4 previously demonstrated for ASUDAS plaques (Nichol and Turner, 1986; Scott and Turner,
5 1997; Scott, 2008; Scott and Irish, 2017). As anticipated, our results highlight some
6 limitations of the use of the current ASUDAS plaque, indicating that it did not necessarily
7 represent an objective gradient of expression of a non-metric tooth feature (Figures 3, 4 and
8 6). Our results also agree with the currently recognized ASUDAS breakpoint between the
9 recorded absence (grades 0-1) and presence (grades 2-7) of shoveling (Scott and Irish, 2017,
10 Scott et al., 2018). This method can also distinguish between the French and South African
11 groups (expressing low degrees of shoveling) and the Chinese sample (being more variable
12 but mostly showing well-defined shovel-shaped incisors). This is in agreement with the vast
13 literature on the topic (e.g., Scott and Turner, 1997; Irish and Scott, 2016; Scott and Irish,
14 2017; Scott et al., 2018) and demonstrates that our method, while confirming the ASUDAS
15 results, opens a path towards more advanced quantitatively-based assessment for the
16 distinction of fossil and extant human populations. This modest sample was only used here to
17 test the method, but by increasing it and incorporating larger chrono-geographic groups,
18 including fossil hominins, there is a high potential to better understand the evolution of
19 shovel-shaped incisors. For example, Neanderthals are well-known for their markedly shovel-
20 shaped incisors and, given the increasing availability of 3D virtual data on their teeth,
21 paleogenetics techniques and molecular data on tooth morphology (Zanolli et al., 2017), this
22 new quantitative method is perfectly suited to the investigation of the evolution of UII
23 shoveling.

24
25
26
27
28
29
30
31
32
33
34
35
36
37 Our protocol integrates the analysis of two different but complementary aspects: the depth
38 of the lingual surface with respect to the marginal ridges and the shape of the lingual aspect.
39 This is an important point as our analyses have revealed that visual rating of shoveling tends
40 to be more prone to intra- and inter-observer bias for the highest grades (even starting at grade
41 2). In addition, even when the observers are well trained and follow the definition of the UII
42 shoveling trait (Supporting Information Table 2), when dealing with numerous specimens,
43 they tend to create a mental image of the ASUDAS categories and then make their judgments,
44 resulting in a mental scale that is linearly dependent on the maximum depth of the palatal
45 aspect, while the ASUDAS grades are not distributed linearly for this parameter. This results
46 in the visually assigned ratings being correlated with the maximum depth rather than with
47 predicted ASUDAS categories. In this context, our results provide a reliable, reproducible
48 framework reinforced by statistical results supporting the fact that open scale numerical
49 measurements can complement the ASUDAS method and provide new information. Of
50
51
52
53
54
55
56
57
58
59
60

1
2
3 course, similar methods complementing the classic ASUDAS method still need to be
4 developed for other non-metric dental traits. There are also other possibilities for the
5 quantitative study of shape variation, with or without landmarks. For example, a surface
6 deformation-based approach considering a 3D portion of the crown surface (such as the
7 lingual aspect in the case of UI1 shoveling) could be used to assess the degree of deformation
8 from one tooth to another and quantify shape variations of the complete set of dental traits
9 (Durrleman et al., 2012; Durrleman et al., 2014). Thus, although the ASUDAS is a reliable and
10 efficient tool, it is still possible to complement it with alternative methods.
11
12
13
14
15

16 17 **Acknowledgements**

18 This study is based on the PhD research program of the first author. It is supported by the
19 French CNRS. The work of P. Monsarrat is supported by Toulouse University Hospital (CHU
20 de Toulouse), Université Toulouse III - Paul Sabatier, the Midi-Pyrénées region and the
21 research platform of the Toulouse Dental Faculty (PLTRO). J. Braga provided access to the
22 ASUDAS plaque. We thank G. Krüger for granting access to the Pretoria Bone Collection
23 (PBC) used in this study. For scientific discussion, we are also grateful to F. Duret.
24
25
26
27
28
29

30 31 **References**

- 32 Altman, D.G. (2006). The cost of dichotomising continuous variables. *The British Medical*
33 *Journal*, **332**, 1080.
34
35 Bailey, S.E., & Wood, B.A. (2007). Trends in postcanine occlusal morphology within the
36 hominin clade: the case of *Paranthropus*. In S.E. Bayley & J.-J. Hublin (Eds.), *Dental*
37 *Perspectives on Human Evolution: State of the Art Research in Dental Anthropology* (pp.
38 33-52). Dordrecht: Springer.
39
40 Bailey, S.E., & Hublin J.-J. (2013). What does it mean to be dentally “modern”? In G.R. Scott
41 & J.D. Irish (Eds.), *Anthropological Perspectives on Tooth Morphology, Genetics,*
42 *Evolution, Variation* (pp. 222-249). Cambridge: Cambridge University Press.
43
44 Bhandari, M., Lochner, H., & Tornetta P. (2002). Effect of continuous versus dichotomous
45 outcome variables on study power when sample sizes of orthopaedic randomized trials are
46 small. *Archives of Orthopaedic and Trauma Surgery*, **122**, 96-98.
47
48 Carbonell, V.M. (1963). Variations in the frequency of shovel-shaped incisors in different
49 populations. In D.R. Brothwell (Ed.), *Dental Anthropology* (pp. 211-234). New York:
50 Pergamon Press.
51
52
53
54
55
56
57
58
59
60

- 1
2
3 Carter, K., Worthington, S., & Smith, T. (2014). Non-metric dental traits and hominin
4 phylogeny. *Journal of Human Evolution*, **69**, 123-128.
- 5
6 Coleman, M.N., & Colbert, M.W. (2007). CT thresholding protocols for taking measurements
7 on three-dimensional models. *American Journal of Physical Anthropology*, **133**, 723-725.
- 8
9 Crummett, T. (1994). *The evolution of shovel shaping: regional and temporal variation in*
10 *human incisor morphology*. Ph.D. Dissertation, University of Michigan, Ann Arbor.
- 11
12 Crummett, T. (1995). The three dimensions of shovel-shaping. In J. Moggi-Cecchi (Ed.),
13 *Aspects of Dental Biology: Palaeontology, Anthropology and Evolution* (pp. 305-313).
14 Florence: International Institute for the Study of Man.
- 15
16
17 Dahlberg, A.A. (1956). *Materials for the Establishment of Standards for Classification of*
18 *Tooth Characteristics, Attributes, and Techniques in Morphological Studies of the*
19 *Dentition*. Chicago: Zoller Laboratory of Dental Anthropology, University of Chicago.
- 20
21
22 Dahlberg, A.A. & Mikkelsen, O. (1947). The shovel-shaped character in the teeth of the Pima
23 Indians. *American Journal of Physical Anthropology*, **5**, 234-235.
- 24
25
26 Denton, L.C. (2011). *Shovel-Shaped Incisors and the Morphology of the Enamel-Dentin*
27 *Junction: An Analysis of Human Upper Incisors in Three Dimensions*. Master dissertation,
28 Colorado State University, Fort Collins.
- 29
30
31 Donner, A., & Eliasziw, M. (1994). Statistical implications of the choice between a
32 dichotomous or continuous trait in studies of interobserver agreement. *Biometrics*, **50**, 550-
33 555.
- 34
35
36 Dray, S. & Dufour, A.B. (2007). The ade4 package: implementing the duality diagram for
37 ecologists. *Journal of Statistical Software*, **22**, 1-20.
- 38
39
40 Dryden, I.L. (2017). shapes package. R Foundation for Statistical Computing, Vienna,
41 Austria. Contributed package. Version 1.2.3. URL <http://www.R-project.org>.
- 42
43
44 Durrleman, S., Prastawa, M., Korenberg, J.R., Joshi, S., Trouvé, A., & Gerig, G. (2012).
45 Topology preserving atlas construction from shape data without correspondence using
46 sparse parameters. In N. Ayache, H. Delingette, P. Golland & K. Mori (Eds.), *Proceedings*
47 *of Medical Image Computing and Computer Aided Intervention* (pp. 223-230). Nice:
48 Springer.
- 49
50
51 Durrleman, S., Prastawa, M., Charon, N., Korenberg, J.R., Joshi, S., Gerig, G., & Trouvé, A.
52 (2014). Morphometry of anatomical shape complexes with dense deformations and sparse
53 parameters. *NeuroImage*, **101**, 35-49.
- 54
55
56
57
58
59
60

- 1
2
3 Fajardo, R.J., Ryan, T.M., & Kappelman J. (2002). Assessing the accuracy of high-resolution
4 X-ray computed tomography of primate trabecular bone by comparisons with histological
5 sections. *American Journal of Physical Anthropology*, **118**, 1-10.
- 6
7
8 Gamer, M., Lemon, J., & Puspendra Singh, I. (2012). irr: Various Coefficients of Interrater
9 Reliability and Agreement. R package version 0.84. [https://CRAN.R-](https://CRAN.R-project.org/package=irr)
10 [project.org/package=irr](https://CRAN.R-project.org/package=irr).
- 11
12 Goaz, P.W., & Miller, M.C. (1966). A preliminary description of the dental morphology of
13 the Peruvian Indians. *Journal of Dental Research*, **45**, 106-119.
- 14
15
16 Hanihara, K. (1969). Mongoloid dental complex in the permanent dentition. *Proceedings of*
17 *the VIIIth International Congress of Anthropological and Ethnological Sciences*, **1**, 298-
18 300.
- 19
20
21 Hanihara, K., Masuda, T., Tanaka, T. (1975). Family studies of the shovel trait in the
22 maxillary central incisor. *Journal of the Anthropological Society of Nippon*, **83**, 107-12.
- 23
24
25 Hanihara, K. (2008). Morphological variation of major human populations based on
26 nonmetric dental traits. *American Journal of Physical Anthropology*, **136**, 169-182.
- 27
28
29 Hillson, S.W. (1996). *Dental anthropology*. Cambridge: Cambridge University Press.
- 30
31
32 Hillson, S.W. (2005). *Teeth*. Cambridge: Cambridge University Press.
- 33
34
35 Hlusko, L.J., Carlson, J.P., Chaplin, G., Elias, S.A., Hoffecker, J.F., Huffman, M., Jablonski,
36 N.G., Monson, T.A., O'Rourke, D.H., Pilloud, M.A., & Scott, G.R. (2018). Environmental
37 selection during the last ice age on the mother-to-infant transmission of vitamin D and fatty
38 acids through breast milk. *Proceedings of the National Academy of Sciences of the United*
39 *States of America* (in press, doi.org/10.1073/pnas.1711788115).
- 40
41
42 Hoffman, J.W., & de Beer, F.C. (2012) Characteristics of the Micro-Focus X-ray
43 Tomography Facility (MIXRAD) at Necsas in South Africa. In *Proceedings of the 18th*
44 *World Conference on Nondestructive Testing* (pp. 1-12). Durban: South African Institute
45 for Non-Destructive Testing.
- 46
47
48 Hrdlička, A. (1920). Shovel-shaped teeth. *American Journal of Physical Anthropology*, **3**,
49 429-465.
- 50
51
52 Hughes, I., & Hase, T. (2010). *Measurements and Their Uncertainties: A Practical Guide to*
53 *Modern Error Analysis*. Oxford: Oxford University Press.
- 54
55
56 Irish, J.D. (1998). Ancestral dental traits in recent Sub-Saharan Africans and the origins of
57 modern humans. *Journal of Human Evolution*, **34**, 81-98.
- 58
59
60

- 1
2
3 Irish, J.D., & Guatelli-Steinberg, D. (2003). Ancient teeth and modern human origins: An
4 expanded comparison of African Plio-Pleistocene and recent world dental samples.
5 *Journal of Human Evolution*, **45**, 113-144.
6
7 Irish, J.D., Guatelli-Steinberg, D., Legge, S.S., Ruitter, D.J., & Berger, L.R. (2013). Dental
8 morphology and the phylogenetic “place” of *Australopithecus sediba*. *Science*, **340**,
9 1233062.
10
11 Irish, J.D. (2014). Dental nonmetric variation around the world: Using key traits in
12 populations to estimate ancestry in individuals. In G.E. Berg & S.C. Ta'ala (Eds.),
13 *Biological Affinity in Forensic Identification of Human Skeletal Remains: Beyond Black*
14 *and White* (pp. 165-190). Boca Raton: CRC Press-Taylor and Francis Group.
15
16 Irish, J.D., Guatelli-Steinberg, D., Legge, S.S., Ruitter, D.J., & Berger, L.R. (2014). Response
17 to “Non-metric dental traits and hominin phylogeny” by Carter et al., with additional
18 information on the Arizona State University Dental Anthropology System and
19 phylogenetic “place” of *Australopithecus sediba*. *Journal of Human Evolution*, **69**, 129-
20 134.
21
22 Irish, J.D., & Scott, G.R. (2016). *A Companion to Dental Anthropology*. Chichester: Wiley
23 Blackwell.
24
25 Jernvall, J., Keränen, S.V.E., & Thesleff, I. (2000). Evolutionary modification of development
26 in mammalian teeth: Quantifying gene expression patterns and topography. *Proceedings of*
27 *the National Academy of Sciences of the United States of America*, **97**, 14444–14448.
28
29 Joint Committee for Guides in Metrology. (2008). *The International Vocabulary of*
30 *Metrology, Basic and General Concepts and Associated Terms*.
31
32 Kimura, R., Yamaguchi, T., Takeda, M., Kondo, O., Toma, T., Haneji, K., Hanihara, T.,
33 Matsukusa, H., Kawamura, S., Maki, K., Osawa, M., Ishida, H., & Oota, H. (2009). A
34 common variation in EDAR is a genetic determinant of shovel shaped incisors. *The*
35 *American Journal of Human Genetics*, **85**, 528-535.
36
37 Koo, T.K., Li, M.Y. (2017). A guideline of selecting and reporting intraclass correlation
38 coefficients for reliability research. *Journal of Chiropractic Medicine*, **15**, 155-163.
39
40 Le Cabec, A., Gunz, P., Kupczik, K., Braga, J., & Hubin, J.J. (2013). Anterior tooth root
41 morphology and size in Neanderthals: taxonomic and functional implications. *Journal of*
42 *Human Evolution*, **64**, 169-193.
43
44 Lehnert, B. (2015). BlandAltmanLeh package. R Foundation for statistical computing,
45 Vienna, Austria. Contributed package. Version 0.3.1. Available from: [http://www.R-](http://www.R-project.org)
46 [project.org](http://www.R-project.org).
47
48
49
50
51
52
53
54
55
56
57
58
59
60

- 1
2
3 Ligges, U., & Mächler, M. (2003). Scatterplot3d - an R Package for Visualizing Multivariate
4 Data. *Journal of Statistical Software*, **8**, 1-20.
- 5
6 MacCallum, R.C., Zhang, S., Preacher, K.J., & Rucker, D.D. (2002). On the practice of
7 dichotomization of quantitative variables. *Psychological Methods*, **7**, 19-40.
- 8
9 Martínón-Torres, M., Bermúdez de Castro, J.M., Gómez-Robles, A., Arsuaga, J.L., Carbonell,
10 E., Lordkipanidze, D., Manzi, G., & Margvelashvili, A. (2007). Dental evidence on the
11 hominin dispersals during the Pleistocene. *Proceedings of the National Academy of*
12 *Sciences of the United States of America*, **104**, 13279-13282.
- 13
14
15
16 MATLAB and Statistics Toolbox Release. (R2017ba). The MathWorks, Inc., Natick,
17 Massachusetts, United States.
- 18
19 Mizogushi, Y. (1985). Shovelings: a statistical analysis of its morphology. *The University*
20 *Museum, the University of Tokyo Bulletin*, **26**.
- 21
22 Mizogushi, Y. (2013). Significant among-population associations found between dental
23 characters and environmental factors. In G.R. Scott & J.D. Irish (Eds.), *Anthropological*
24 *Perspectives on Tooth Morphology, Genetics, Evolution, Variation* (pp. 108-125).
25 Cambridge: Cambridge University Press.
- 26
27
28
29 Nichol, C.R., & Turner, C.G., II (1986). Intra- and interobserver concordance in classifying
30 dental morphology. *American Journal of Physical Anthropology*, **69**, 299-315.
- 31
32 Park, J.H., Yamaguchi, T., Watanabe, C., Kawaguchi, A., Haneji, K., Takeda, M., Kim, Y.I.,
33 Tomoyasu, Y., Watanabe, M., Oota, H., Hanihara, T., Ishida, H., Maki, K., Park, A.B., &
34 Kimura, R. (2012). Effects of an Asian-specific nonsynonymous EDAR variant on
35 multiple dental traits. *Journal of Human Genetics*, **57**, 508-514.
- 36
37
38
39 Pilbrow, V. (2003). *Dental variation in African apes with implications for understanding*
40 *patterns of variation in species of fossil apes*. PhD Dissertation. New York: University of
41 New York.
- 42
43
44 R Core Team. (2017). R Foundation for statistical computing. Vienna, Austria. Version 3.4.3.
45 Available from: <http://www.R-project.org>.
- 46
47 Salazar-Ciudad, I. & Jernvall, J. (2002). A gene network model accounting for development
48 and evolution of mammalian teeth. *Proceedings of the National Academy of Sciences of the*
49 *United States of America*, **99**, 8116-8120.
- 50
51 Salazar-Ciudad, I. & Jernvall, J. (2010). A computational model of teeth and the
52 developmental origins of morphological variation. *Nature*, **464**, 583-586.
- 53
54
55
56
57
58
59
60

- 1
2
3 Scott, G.R (1973). *Dental Morphology: a genetic study of American White Families and*
4 *Variation in living Southwest Indians*. PhD dissertation, Department of Anthropology,
5 Arizona State University, Tempe.
6
7 Scott, G.R. (2008). Dental Morphology. In A. Katzenburg & S. Saunders (Eds.), *Biological*
8 *Anthropology of the Human Skeleton, 2nd Edition* (pp. 265-298). New York: Wiley-Liss.
9
10 Scott, G.R., & Irish, J.D. (2017). *Human Tooth Crown and Root Morphology. The Arizona*
11 *State University Dental Anthropology System*. Cambridge: Cambridge University Press.
12
13 Scott, G.R., & Turner, C.G. (1997). *The Anthropology of Modern Human Teeth: Dental*
14 *Morphology and its Variation in Recent Human Populations, 2nd Edition*. Cambridge:
15 Cambridge University Press.
16
17 Scott, G.R., Turner, C.G., Townsend, G.C., & Martínón-Torres, M. (2018). *The Anthropology*
18 *of Modern Human Teeth. Dental Morphology and Its Variation in Recent and Fossil Homo*
19 *sapiens*. Cambridge: Cambridge University Press.
20
21 ShROUT, P.E., & Fleiss, J.L. (1979). Intraclass correlations: Uses in assessing rater reliability.
22 *Psychological Bulletin*, **86**, 420-428
23
24 Smith, H. B. (1984). Patterns of molar wear in hunter-gatherers and agriculturalists. *American*
25 *Journal of Physical Anthropology*, **63**, 39-56.
26
27 Spoor, C.F., Zonneveld, F.W., & Macho, G.A. (1993). Linear measurements of cortical bone
28 and dental enamel by computed tomography: Applications and problems. *American*
29 *Journal of Physical Anthropology*, **91**, 469-484.
30
31 Taverne, P.P., Amesz-Voorhoeve, W.H.M., Leertouwer, H.L. (1979). A photogrammetric
32 method which provides geometric data in dental morphology. *Zeitschrift fur Morphologie*
33 *und Anthropologie*, **70**, 163-173.
34
35 Turner, II C.G. (1990). Major features of sundadonty and sinodonty, including suggestions
36 about East Asian microevolution, population history, and Late Pleistocene relationships
37 with Australian aboriginals. *American Journal of Physical Anthropology*, **82**, 295-317.
38
39 Turner, II C.G., Nichol, C.R., & Scott, G.R. (1991). Scoring procedures for key
40 morphological traits of the permanent dentition: the Arizona State University Dental
41 Anthropology System. In M.A. Kelley & C.S. Larsen (Eds.), *Advances in Dental*
42 *Anthropology* (pp. 13-31). New York, Wiley-Liss.
43
44 Zanolli, C. (2013). Additional evidence for morpho-dimensional tooth crown variation in a
45 new Indonesian *H. erectus* sample from the Sangiran Dome (Central Java). *PLoS One*, **8**,
46 e67233.
47
48
49
50
51
52
53
54
55
56
57
58
59
60

1
2
3 Zanolli, C., Bondioli, L., Coppa, A., Dean, M.C., Bayle, P., Candilio, F., Capuani, S., Dreossi,
4 D., Fiore, I., Frayer, D.W., Libsekal, Y., Mancini, L., Rook, L., Medin, T., Tuniz, C., &
5 Macchiarelli, R. (2014). The late Early Pleistocene human dental remains from Uadi Aalad
6 and Mulhuli-Amo (Buia), Eritrean Danakil: macromorphology and microstructure. *Journal*
7 *of Human Evolution*, **74**, 96-113.

8
9
10
11 Zanolli, C., Hourset, M., Esclassan, R., & Mollereau, C. (2017). Neanderthal and Denisova
12 tooth protein variants in present-day humans. *PLoS One*, **12**, e0183802.
13
14
15
16
17
18
19
20
21
22
23
24
25
26
27
28
29
30
31
32
33
34
35
36
37
38
39
40
41
42
43
44
45
46
47
48
49
50
51
52
53
54
55
56
57
58
59
60

Captions for figures

Figure 1. (a). Position of the reference plane located at the midpoint of the crown, which was used to place the semilandmarks along the curve of the lingual aspect of the crown from the mesial to the distal side (b). The maxima of the extreme curvature line were used as starting and ending points of our GM analysis

Figure 2. Illustration of the maximum depth and hollow area (a) used in the non-Procrustes analyses (semilandmark curves aligned with their first and last points). The ASUDAS reference plaque teeth curves are superimposed following this non-Procrustes approach, showing the non-linear variation in shape from grade 0 to grade 6 (b).

Figure 3. Principal component analysis (PCA) of the Procrustes-registered shape coordinates of the 100 semilandmarks used as proxy to assess UI1 shoveling. A: PC1 vs. PC2; B: PC3 vs. PC4.

Figure 4. Histograms showing the frequency of Procrustes PC1 (a), maximum depth (b) and hollow area (c) values for the 87 modern human specimens and the distribution of the ASUDAS reference grades (black vertical lines).

Figure 5. Bland-Altman visualization for agreement of the ASUDAS visual observations and Procrustes coordinates of the semilandmark curves. The different agreements between the two raters were plotted for X, Y and Z float coordinates. Among the 100 landmarks, only the first, mid and last landmarks are drawn.

Figure 6. Plots of the maximum depth against the visual ASUDAS scoring of the first observer's tests (VS1 T1: a; VS1 T2: b) and the second rater (VS2: c). The black dots correspond to the values of the ASUDAS reference plaque and they were joined up via spline interpolation. The symbols represent the chrono-geographic origin as indicated in the legend of the graphs.

1
2
3
4
5
6
7
8
9
10
11
12
13
14
15
16
17
18
19
20
21
22
23
24
25
26
27
28
29
30
31
32
33
34
35
36
37
38
39
40
41
42
43
44
45
46
47

Table 1. List of 87 modern human UI1 elements considered in this study.

Time period	Geographic origin	depository
contemporary (n=13)	France	MHNT ¹
medieval(n=31)	France	INRAP ²
contemporary (n=13)	China	IVPP ³
contemporary (n=30)	South Africa	PBC ⁴

¹MHNT: Natural History Museum of Toulouse; ²INRAP: French National Institute for Preventive Archeological Research; ³IVPP: Institute of Vertebrate Paleontology and Paleoanthropology of Beijing; ⁴PBC: Pretoria Bone Collection of the Department of Anatomy of the University of Pretoria, representing individuals of various ancestries including Nbele, N Sotho, Swazi and Zulu.

Table 2. Intra-Class Correlation (ICC) values for intra-observer (VS1 T1 vs. T2) and inter-observer (VS1 vs. VS2) consistency measures and accuracy (comparing the three ratings with their predicted values from the ASUDAS reference plate teeth). Shades of color represent the degree of consistency and accuracy, with darker green corresponding to the highest degrees and white to the lowest degree.

	consistency (precision)		accuracy (unbiasedness)		
	VS1 T1 vs T2	VS1 vs VS2	VS1 T1 vs predicted	VS1 T2 vs predicted	VS2 vs predicted
all samples	0.985	0.987	0.759	0.749	0.772
South African	0.946	0.986	0.602	0.565	0.602
French contemporary	0.900	0.721	0.496	0.570	0.494
French medieval	0.971	0.993	0.550	0.592	0.559
Chinese	0.976	0.975	0.000	0.000	0.000

1
2
3
4
5
6
7
8
9
10
11
12
13
14
15
16
17
18
19
20
21
22
23
24
25
26
27
28
29
30
31
32
33
34
35
36
37
38
39
40
41
42
43
44
45
46
47

Table 3. Correlations between various measurements obtained from the coordinates of all samples (87 human specimens plus the 7 ASUDAS reference casts). Maximum depth and hollow area are the directly measured metrics based on the non-Procrustes alignment method. Principal components were obtained from both Procrustes and non-Procrustes methods. Shades of color represent the degree of correlation, with darker green corresponding to the highest degrees and white to the lowest degree. Red indicates negative correlation.

		direct metrics		Procrustes PC		non-Procrustes PC	
		maximum depth	hollow area	PC1	PC2	PC1	PC2
direct metrics	maximum depth	-	0.98	0.98	0.08	0.99	-0.08
	hollow area	0.98	-	0.96	0.20	1.00	0.06
Procrustes PC	PC1	0.98	0.96	-	0.00	0.97	-0.21
	PC2	0.08	0.20	0.00	-	0.16	0.86
non-Procrustes PC	PC1	0.99	1.00	0.97	0.16	-	0.00
	PC2	-0.08	0.06	-0.21	0.86	0.00	-

Table 4. Correlation of observer-assigned ASUDAS categories with the predicted ASUDAS value, the first four PCs of the Procrustes analysis, the maximum palatal depth and the hollow area. Shades of color represent the degree of correlation, with darker green corresponding to the highest degrees and white to the lowest degree. Red indicates negative correlation.

	VS1 T1	VS1 T2	VS2
predicted ASUDAS	0.776	0.769	0.788
PC1	0.836	0.831	0.850
PC2	0.153	0.169	0.177
PC3	-0.106	-0.097	-0.082
PC4	0.055	0.028	0.056
maximum depth	0.840	0.833	0.852
hollow area	0.832	0.828	0.848

1
2
3
4
5
6
7
8
9
10
11
12
13
14
15
16
17
18
19
20
21
22
23
24
25
26
27
28
29
30
31
32
33
34
35
36
37
38
39
40
41
42
43
44
45
46
47

Table 5. ICC values for intra-observer (VS1 T1 vs. T2) and inter-observer (VS1 vs. VS2) consistency measures and accuracy (comparing the three ratings with their predicted values from the ASUDAS reference plate teeth) when grades 0-1 and 2-6 are fused into two groups (2-category split). Shades of color represent the degree of consistency and accuracy, with darker green corresponding to the highest degrees and white to the lowest degree.

	consistency (precision)		accuracy (unbiasedness)		
	VS1 T1 vs T2	VS1 vs VS2	VS1 T1 vs predicted	VS1 T2 vs predicted	VS2 vs predicted
all samples	0.945	0.964	0.812	0.827	0.842

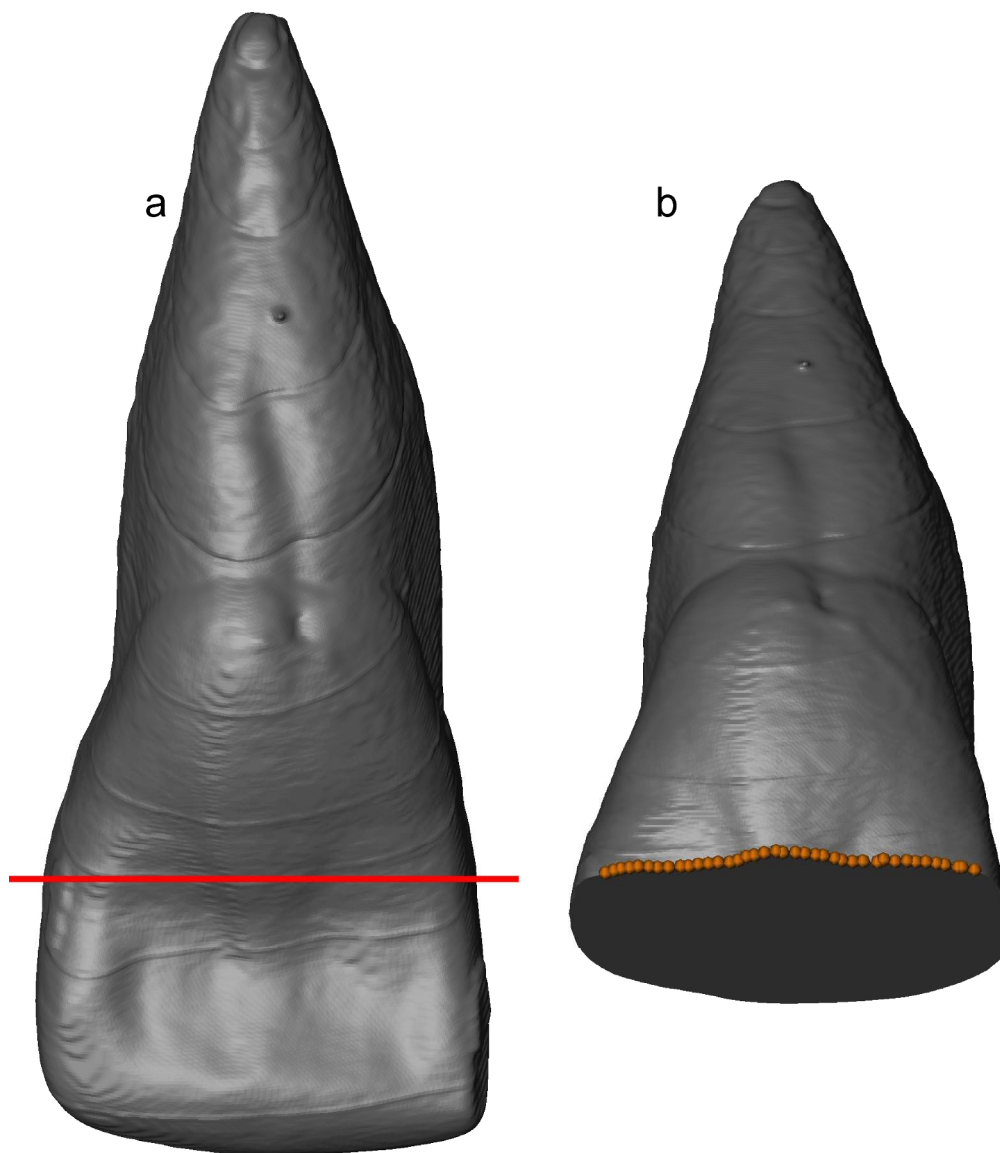


Figure 1. (a). Position of the reference plane located at the midpoint of the crown, that is used to put the semilandmarks along the curve of the lingual aspect of the crown from mesial to distal side. (b). We use the maxima of the extreme curvature line as starting and ending points of our GM analysis.

356x407mm (300 x 300 DPI)

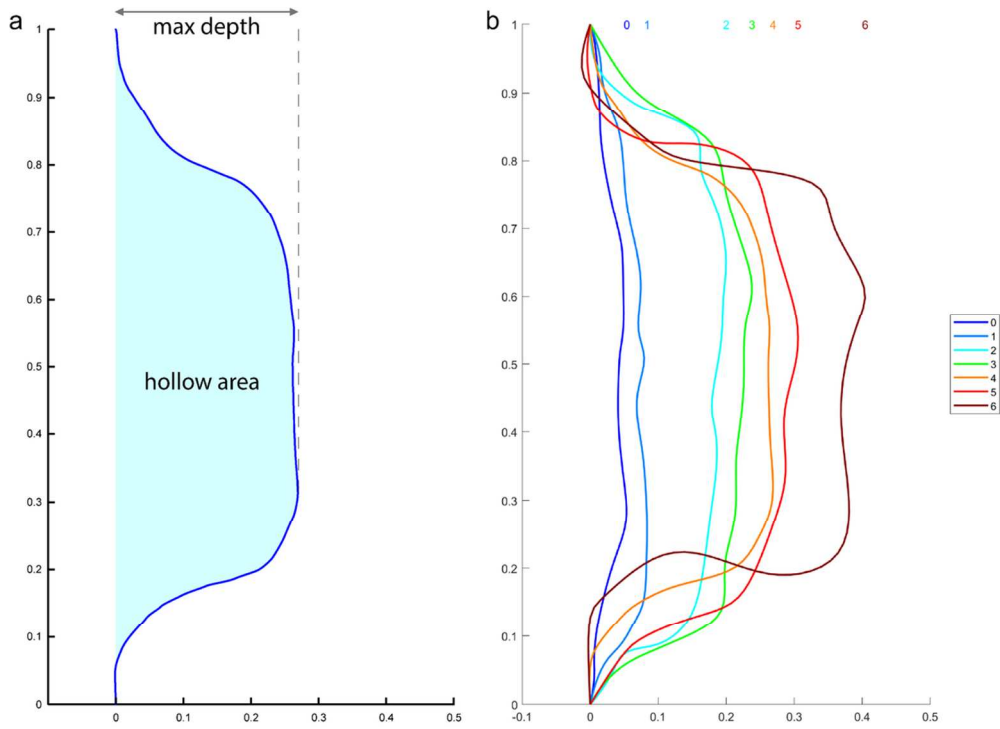


Figure 2. Illustration of the maximal depth and hollow area (a) used in the non-Procrustes analyses (semilandmark curves aligned with their first and last points). The ASUDAS reference plaque teeth curves are superimposed following this non-Procrustes approach, showing the non-linear variation in shape from grade 0 to grade 6 (b).

106x76mm (300 x 300 DPI)

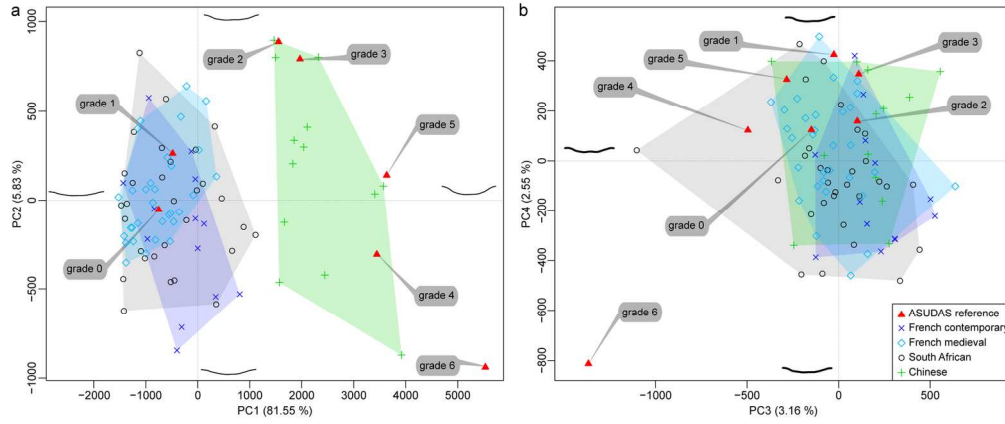


Figure 3. Principal component analysis (PCA) of the Procrustes-registered shape coordinates of the 100 semilandmarks used as proxy to assess UI1 shoveling. A: PC1 vs. PC2; B: PC3 vs. PC4.

154x64mm (300 x 300 DPI)

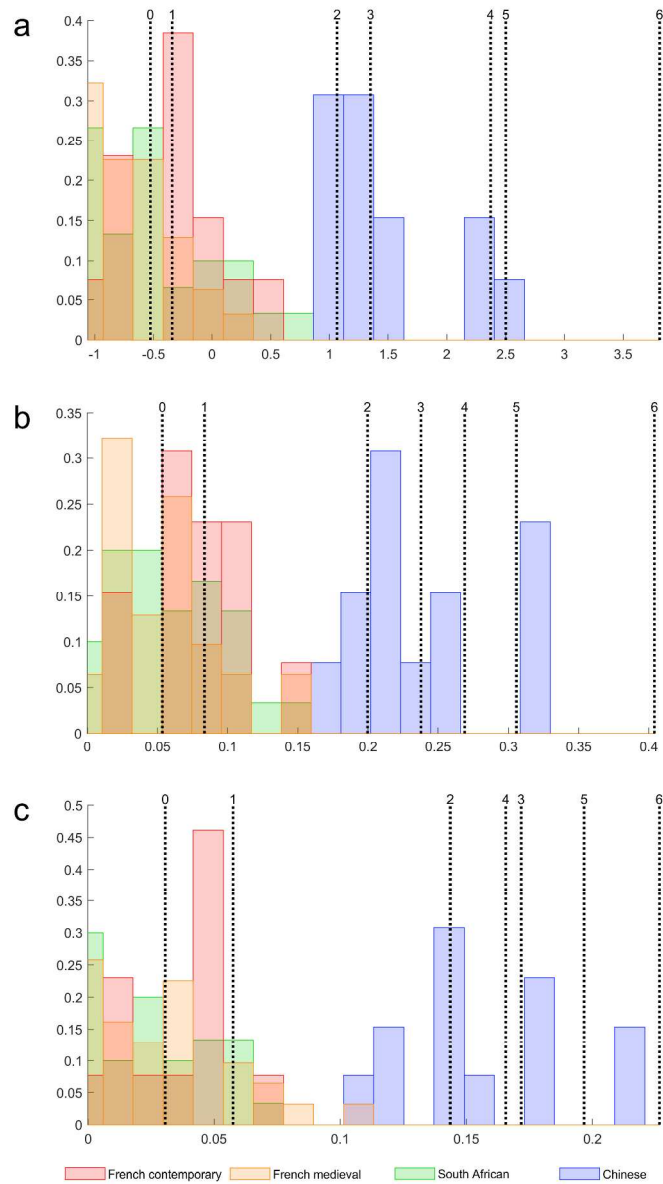


Figure 4. Histograms showing the frequency of Procrustes PC1 (a), maximum depth (b) and hollow area (c) values for the 87 modern human specimens and the distribution of the ASUDAS reference grades (black vertical lines).

187x319mm (300 x 300 DPI)

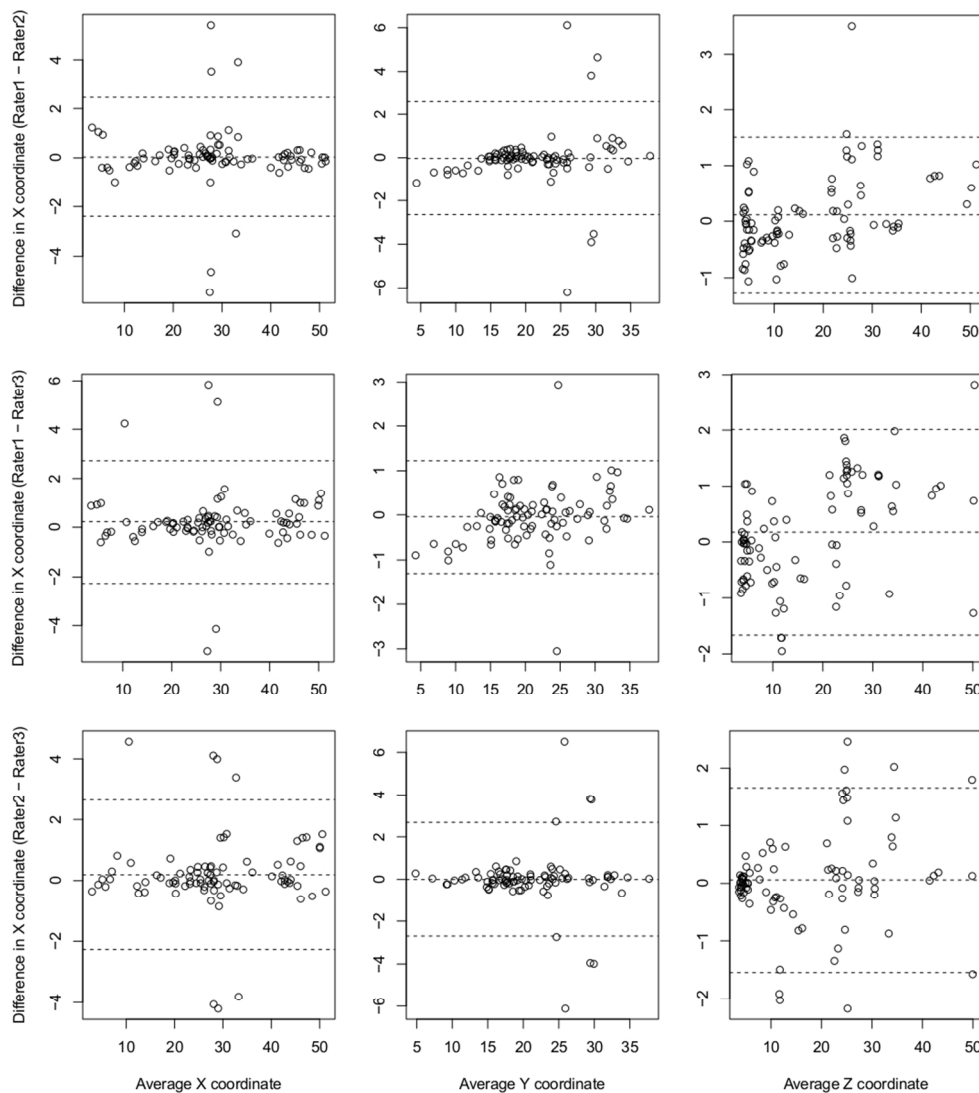


Figure 5. Bland-Altman visualization for agreement of the ASUDAS visual observations and Procrustes coordinates of the semilandmark curves. The different agreements among the pair of raters were plotted for X, Y and Z float coordinates. Among the 100 landmarks, only first, mid and last landmarks were drawn.

92x103mm (300 x 300 DPI)

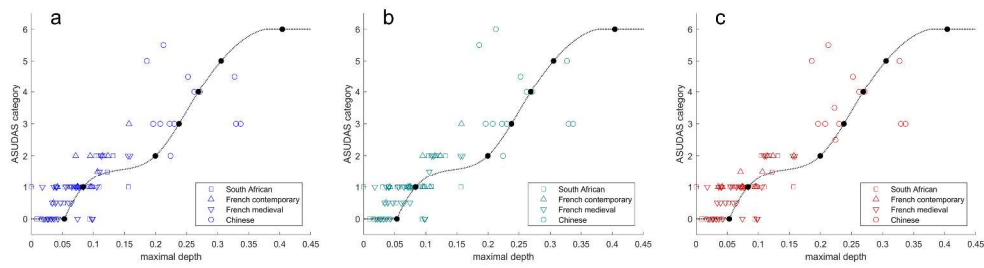


Figure 6. Plots of the maximum depth against the visual ASUDAS scoring of the first observer's tests (VS1 T1: a; VS1 T2: b) and the second rater (VS2: c). The black dots correspond to the values of the ASUDAS reference plaque and they joined between them via spline interpolation. The symbols represent the chrono-geographic origin as indicated in the legend of the graphs.

411x111mm (300 x 300 DPI)